Landslide Susceptibility Assessment Using the Analytic Hierarchy Process (AHP): A Case Study of Al Figrah Road, Al-Madinah, Saudi Arabia

Talal Alharbi *, Abdelbaset S. El-Sorogy *, Khaled Al-Kahtany, Yousef Salem, Naji A. Rikan

Posted Date: 15 October 2024

doi: 10.20944/preprints202410.1125.v1

Keywords: landslide; remote sensing; Geographic Information System; Analytical Hierarchy Process (AHP); Saudi Arabia

 doi:10.20944/preprints202410.1125.v1

Article

Landslide Susceptibility Assessment Using the Analytic Hierarchy Process (AHP): A Case Study of Al Figrah Road, Al-Madinah, Saudi Arabia

Talal Alharbi, Abdelbaset S. El-Sorogy *, Khaled Al-Kahtany, Yousef Salem and Naji Rikan

Geology and Geophysics Department, College of Science, King Saud University, Riyadh 11451, Saudi Arabia
* Correspondence: asmohamed@ksu.edu.sa

Abstract: Landslides in the hilly regions of Al-Madinah Al-Munawarah are a natural hazard that endangers both infrastructure and human lives. The objective of this work is to create maps that show the likelihood of landslides occurring on the Al Figrah Road, which is a vital road connects the cities of Al-Madinah and Yanbu. This will be done using the analytical hierarchy process (AHP) approach. The landslide susceptibility maps have been created by taking into account various parameters such as elevation, slope, aspect, drainage density, lithology, soil, and precipitation. Assess the significance of these thematic layers in relation to the frequency of landslides in the research area based on historical landslide data and field verification, in order to allocate suitable weights. The sensitivity maps of the study region delineated areas with low risk (93,552,333 m^2), moderate risk (271,180,722 m^2), and high risk (33,053,839 m^2). 28.63% of the Al Figrah total Road is classified as low risk, 48.09% as moderate risk, and 23.28% as high risk. A total of 10 landslides were identified in areas with steep slopes and denudational hills, confirming the findings of the AHP analysis conducted in high-risk zones. The integrity of these slide zones was greatly impacted by the presence of joints, faults, foliation, and shear zones within igneous and metamorphic rocks. Examining the susceptibility of landslides in this region enhances our understanding of landslides on other steep routes in Saudi Arabia.

Keywords: landslide; remote sensing; Geographic Information System; Analytical Hierarchy Process (AHP); Saudi Arabia

1. Introduction

Landslides are geological events that happen in mountainous regions and can cause significant devastation and loss of human life [1]. Landslides occur when rock, mud, or debris moves downward due to the force of gravity [2]. Landslides can be triggered by seismic occurrences, heavy rainfall, rapid melting of snow and ice, or human activities such as infrastructure construction, deforestation, and mining [3]. Rock fall is the most common type of landslide, which occurs when there is a large amount of loose material in hilly or mountainous areas. Landslides are highly destructive and unpredictable, often happening suddenly and without any prior indication [4]. These natural occurrences pose major risks to the welfare of nearby residents and infrastructure, potentially causing economic harm. Hence, doing comprehensive analysis is vital to minimize harm and prevent catastrophes [5,6].

Geographic information systems (GIS) and remote sensing data have been used to detect areas that are susceptible to landslides [7]. Various methods have been used in the past to evaluate the probability of landslides happening. The approaches employed encompass the examination of topographical features, the examination of historical instances of landslides, the division of the terrain into distinct zones depending on certain attributes, and the utilization of advanced computer models [8,9]. The methods utilized encompass frequency ratio, the analytical hierarchy process, bivariate and multivariate statistical analyses, logistic regression, artificial neural networks, and fuzzy logic [9–13].

 doi:10.20944/preprints202410.1125.v1

These procedures yield more accurate results when the data is comprehensive and of good quality. This study utilizes the analytic hierarchy process (AHP) to assess the probability of landslides occurring on Al Figrah Road. The AHP is a commonly used heuristic model that integrates qualitative and quantitative methodologies to break down a complex decision problem into several levels. This methodology measures and converts subjective viewpoints into logical decision frameworks [14,15]. This study showcases the efficacy of the AHP in amalgamating many factors such as topography, geological diversity, and climatic fluctuation.

The primary causes of landslides are excavation, mechanical vibration in road network engineering, and changes in land use patterns [15,16]. Landslide susceptibility zoning (LSZ) is the method used to assess the likelihood of a landslide happening in a particular area and visually representing the areas at risk of landslides using a map known as a landslide susceptibility map [17]. Landslide susceptibility zones are often identified by considering factors such as geological processes, soil composition, land elevation, water flow patterns, and human actions that can trigger landslides. These factors are then analyzed using GIS techniques [16,18]. Researchers might explore the correlation between landslides and various causes by analyzing historical data or conducting field studies. This enables them to precisely select pertinent elements and finalize the judgment matrix [19].

Precipitation is a primary factor for landslides globally. Rainwater infiltration into the soil elevates pore-water pressure, diminishing effective stress and shear strength of slope materials, resulting in instability and probable failure [20]. The vulnerability of slopes to rainfall-induced landslides is contingent upon multiple factors, such as rainfall intensity and duration, soil characteristics, slope geometry, and land use practices [21]. The southwestern regions of Saudi Arabia, especially Asir and Jazan, are prone to landslides owing to their hilly topography and seasonal intense precipitation. [22] examined landslides in the Abha area of the Asir region, attributing slope failures to intense precipitation alongside geological and geotechnical influences. Furthermore, [23] conducted a study in the Jazan region, illustrating that severe rainfall events substantially contribute to landslide occurrences.

Several landslides have taken place in the hilly highways of Saudi Arabia, particularly in Al-Baha, Jazan, Al-Madinah, and Makkah. These landslides have resulted in numerous traffic disruptions and have caused multiple disasters [24,25]. The occurrence of landslides has led to substantial road damage, which in turn requires expensive repairs and maintenance that will take several weeks to finish [26]. This study aimed to assess the occurrence of landslide susceptibility on Al Figrah Road in Madinah, Saudi Arabia, using the Analytic Hierarchy Process (AHP) and remote sensing data. The findings of this research will assist policymakers in this region as well as other arid and semi-arid regions in selecting and ranking locations for implementing measures to alleviate and prevent adverse effects.

2. Methodology

2.1. Study Area

The present research area located along Al Figrah Road, a crucial route in the western part of Saudi Arabia, is geographically positioned between coordinates 38°57′ E, 24°18′ N and 39°07′ E, 24°20′ N (Figure 1). This road traverses an area characterized by its diverse elevation, ranging from 795 meters at the valley floor to 1866 meters at top of Al Figrah Mountain. The significant elevation changes along Al Figrah Road present unique challenges for researchers. Many sections of the road are narrow, making it difficult for them to find a suitable starting point for their geological investigations. Such variations in height impact environmental parameters such as temperature and precipitation [27,28], which are critical for the ecological balance of the region. Understanding how elevation influences these factors is vital for assessing and forecasting risks, such as landslides [29,30]. Additionally, this road serves as a strategic shortcut through varied landscapes to Red Sea coast cities like Yanbu.

 doi:10.20944/preprints202410.1125.v1

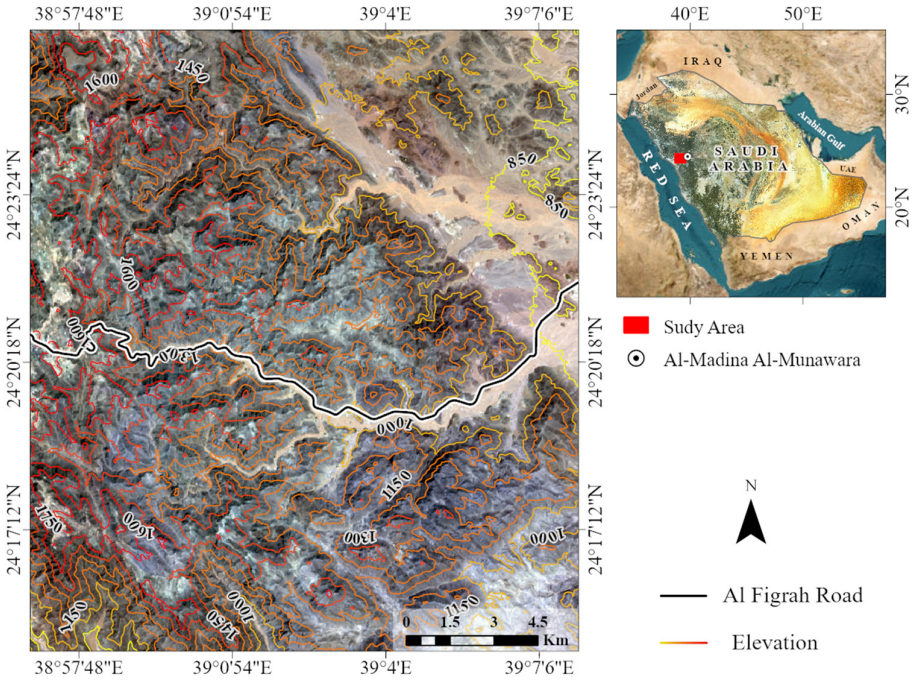

Figure 1. A map displaying Al Figrah Road, which runs through a hilly region with elevation varying from 795 m at the bottom to 1866 m at the mountaintops. The smaller map located in the top right corner provides the study area's location in Saudi Arabia.

The Al Figarh Mountain is part of the Red Sea Mountains, which were formed by the uplifting of Precambrian rock due to Red Sea rifting. Erosion over time has resulted in steep slopes at the edges of the mountain. The region's geological features consist of a variety of rocks, representing its complex geological history. The area is predominantly composed of coarse-grained granite, made up mainly of quartz, feldspar, and mica. Basalt, although less common, is present in volcanic fields and lava flows. The primary metamorphic rocks in the area are schist, which is characterized by well-developed schistocyte and notable gneiss. The region's sedimentary rocks are mainly sandstone and alluvial sediments, composed of sand-sized mineral particles or rock fragments found in valleys. These rocks collectively reflect the diverse geological history of the area, shaped by various tectonic and environmental processes over millions of years [31].

The climatic conditions of this locality exhibit parallels with other territories within the Kingdom of Saudi Arabia, characterized by pronounced diurnal and seasonal thermal oscillations. In the boreal winter, average high temperatures in Medina, where Al Figrah Road is located, are recorded around 24°C in January, while the summer months see temperatures soaring to an average high of 43°C in June [32]. Precipitation patterns in Al Madinah predominantly manifest during the winter, with historical records over the past three decades indicating a range from 3 mm to 90 mm [33]. Orographic influences exerted by the regional topography facilitate pluvial generation, subsequently dispersing across interfluent depressions. The principal fluvial conduits are situated eastward, whereas the orogenic structures delineate the northern, western, and southern peripheries of the study domain.

2.2. Datasets

Utilizing remote sensing and Geographic Information System (GIS) techniques to map landslide susceptibility is an extremely effective method for assessing and evaluating potential landslide risks in designated areas [34]. This method involves collecting, integrating, and analyzing various data types from multiple sources, such as geological, geomorphological, hydrological, and meteorological fields. To delineate landslide susceptibility spatially, datasets like Sentinel-1 satellite imagery and a 12.5-meter digital elevation model (DEM) are employed to extract essential variables, including

 doi:10.20944/preprints202410.1125.v1

drainage density, slope angle, and aspect direction [34]. In addition, it is essential to integrate raster data such as geology, soil type, and precipitation rates to create accurate and reliable landslide susceptibility maps [35]. The process begins with a pre-processing phase where data from geological, geomorphological, hydrological, and meteorological sources is digitized and converted into raster files with constant pixel size. Sentinel-1 derived raster files (including DEM, drainage density, slope, and aspect) are used along with additional datasets like lithology, soil, and precipitation obtained from the Ministry of Environment, Water, and Agriculture.

To develop a landslide risk model, several factors influencing this phenomenon were considered, including slope, rainfall, elevation, drainage density, soil, geology, and slope direction. Each factor was assigned a weight according to its impact on the phenomenon. The Analytical Hierarchy Process (AHP) was employed to estimate and rank the factors controlling landslides. Additionally, mathematical models were used to assess the consistency of the weights assigned to these factors. The AHP is a relative measurement method focusing on how objects compare to one another, specifically how their ratios relate to each other. It offers solutions during modeling processes through pairwise comparisons of factors to indicate the dominance of one factor over another [35]. These pairwise comparisons are arranged in a matrix, referred to as the primary diagonal elements of a reciprocal matrix, which reflects the principle that comparing a factor with itself should yield an equal importance judgment.

The scale of absolute values used to highlight the impact of one factor over another. The AHP analysis facilitated the measurement of consistency levels as an indicator of the consistency ratio (CR) of the weights. This indicator relies on the consistency index (CI) and the random index (RI) in the following equation:

$$CR = CI/RI$$

$$CI = \frac{\lambda_{max} - n}{n - 1}$$

The equation indicates that when the CR value is less than 0.10, the pairwise comparison exhibits acceptable consistency. Conversely, if the CR value is greater than or equal to 0.10, there is inconsistency due to inaccuracies in the pairwise comparison matrix [36]. In this study, the CR value was 0.07, confirming that the weight values were accurate and logical.

Upon completing the risk map, the final phase involves validating the results through field trips (Figure 2). These expeditions assess the high-potential zones identified on the map, ensuring that the theoretical data aligns with the actual conditions on the ground. This step is essential to confirm the accuracy of the risk assessment and to make any necessary adjustments to the map based on empirical evidence [37].

 doi:10.20944/preprints202410.1125.v1

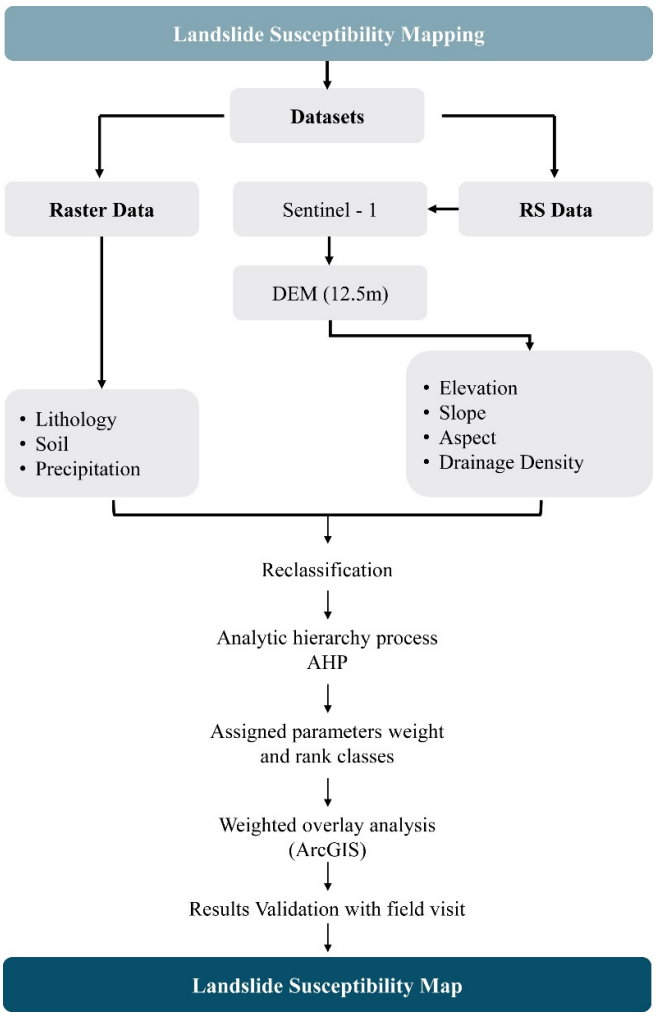

Figure 2. A flow chart outlining how the datasets were utilized to map the potential landslide areas at risk on Al Figrah Road.

Upon completing the risk map, the final phase involves validating the results through field trips. These expeditions assess the high-potential zones identified on the map, ensuring that the theoretical data aligns with the actual conditions on the ground. This step is essential to confirm the accuracy of the risk assessment and to make any necessary adjustments to the map based on empirical evidence [37].

3. Results and Discussion

Although various preventive and mitigated measures to Al Figrah Road, such as enhanced drainage systems, slope stabilization techniques, and early warning systems, have been put in place, the road has consistently experienced periodic landslides since its construction (Figure 3). Spatial analyses can significantly benefit from remote sensing data [38]. To accurately evaluate the risk of landslide, it is essential to use various datasets. This section will cover the datasets used for this purpose, as well as their potential for informing our understanding of landslide risk. Then, we will explore how these datasets can be combined with other raster data sources to create comprehensive models for predicting landslide risks. The datasets that will be examined include drainage density, elevation, slope, precipitation, land use, geology, soil, and aspect.

 doi:10.20944/preprints202410.1125.v1

Figure 3. displays some mitigation measures implemented during the construction and to maintain the Al Figrah Road. (a) Terracing steep slopes can effectively decrease the slope angle and uniformly distribute the load, hence improving stability. (b) Relocate existing land sliding blocks and depressions to the opposite side of the road to prevent traffic interruptions.

3.1. Drainage Density

Drainage density is a measure of the total length of a river or stream network in relation to its surface area. This method is employed to assess the hydrological characteristics of a particular area and can offer direction for decision-making about land use, water management, and environmental conservation [39]. Drainage density is calculated by dividing the total length of all streams and rivers in a specific area by the total surface area of that location. The standard unit of measurement for this is kilometers per square kilometer (km/km²). Examine the correlation between the characteristics of the land and the density of water drainage to determine areas that are prone to landslides [40]. Landslides can happen during periods of intense rainfall when Al-Fiqrah Road joins with drainage or ephemeral streams (Figure 4). The land in the area was categorized into five groups based on the drainage density values: 0–0.90, 1.00–1.50, 1.60–2.10, 2.20–2.80, and 2.90–4.50 km/km² (Figure 4a).

3.2. Topography

The altitude of a region is a crucial determinant in the formation and advancement of landslides, as it directly impacts the velocity at which debris drops and accumulates. Elevated altitudes contribute to increased potential energy, resulting in more rapid and destructive landslides. Moreover, regions located at higher elevations are more susceptible to having steep slopes where debris might accumulate and quickly trigger movement [41]. A digital elevation model (DEM) is a representation of the three-dimensional surface of a terrain, used to map and analyze the topography of a specific area [42]. The research area has a wide range of elevations, with the highest point reaching 1866 meters above mean sea level (AMSL) in the western region and the lowest point measuring 795 meters AMSL in the eastern part. The height of the study area was classified into five distinct categories based on altitude above mean sea level (AMSL): 795–980, 981–1153, 1154–1335, 1336–1524, and 1525–1866 meters AMSL (Figure 4b).

 doi:10.20944/preprints202410.1125.v1

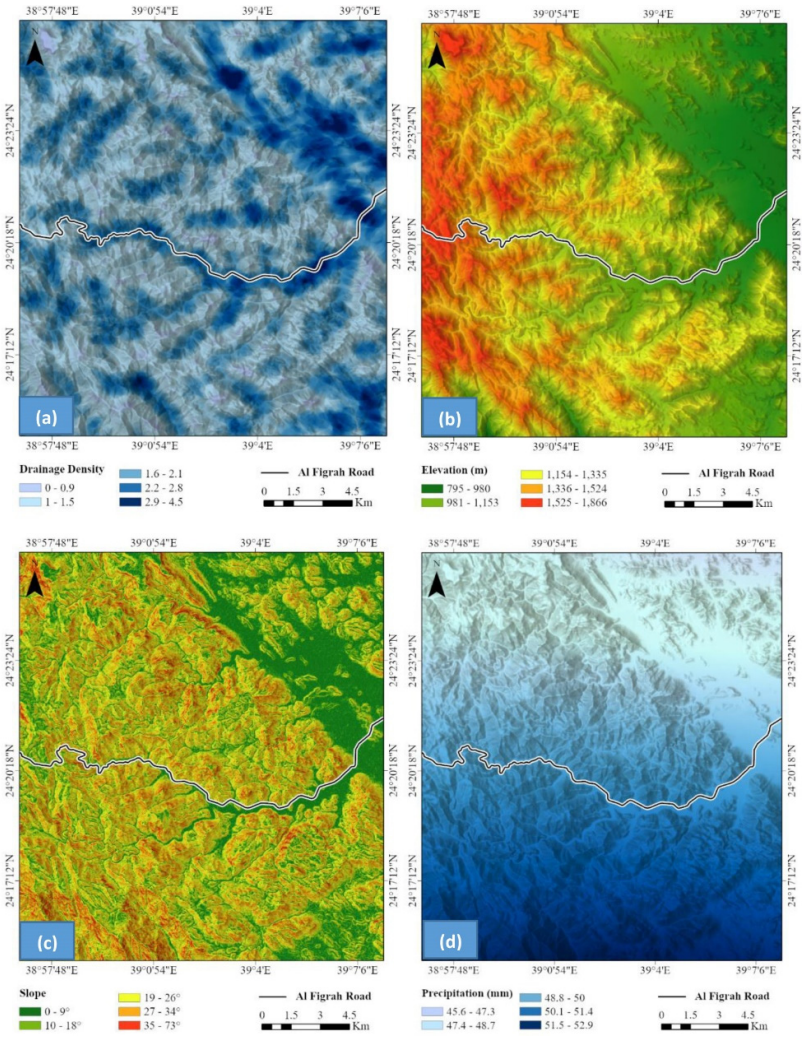

Figure 4. (a) The map displays the five classifications of drainage density in the study region, with values ranging from 0 to 0.90 (km/km²) for the lowest classification and from 2.90 to 4.50 (km/km²) for the highest classification. The junction of ephemeral streams poses a significant risk of landslides on Al Figrah Road. (b) A map depicting the digital portrayal of the surface elevation of the study area, showing a range from 795 to 980 meters above mean sea level (AMSL) in the eastern region and up to 1866 meters AMSL in the western region. (c) A map illustrating the various slopes found in the study areas. The gradient in the lower class ranges from 0 to 9, while in the higher class it spans from 35 to 73. (d) A map illustrating the precise distribution of precipitation levels within the specific area being studied. The highest recorded measurement was 53 mm, while the lowest recorded measurement was 46 mm.

3.3. Slope

In this application, slope refers to formations that exhibit a discernible incline from the horizontal plane [43]. Analyzing the topography of inclined terrain is crucial for understanding the impacts of erosion and sedimentation, as well as the outcomes of human activities on land formations [44]. The slope gradient is a significant aspect that influences the likelihood of landslides, as it greatly affects the speed, path, and destructive potential of landslides *[45,46]*. The study site shown substantial variation in gradient according to its geographical location. The most significant slopes were identified in the mountainous area, mostly in the western section of Al-Fiqrah Road, with a maximum incline of 73°, where a significant number of landslides have taken place. However, areas with sparse vegetation had a greater occurrence of steep slopes, making them more susceptible to

 doi:10.20944/preprints202410.1125.v1

erosion and landslides due to their more prominent inclines. The study region was categorized into five groups based on the slope values: 0 to 9°, 10 to 18°, 19 to 26°, 27 to 34°, and 35 to 73° (Figure 4c).

3.4. Annual Precipitation

Madinah Al Minawarrah experiences a dry environment with increased annual rainfall occurring from November to January. The annual maximum precipitation in Al Figrah Road and its vicinity, particularly the southern region, amounts to 52.9 mm. The research area exhibits little fluctuations in the annual precipitation rate. The data was categorized into five intervals: 45.6–47.3, 47.4–48.7, 48.8–50.0, 50.1–51.4, and 51.5–52.9 mm/year (Figure 4d). Rainwater penetration into rock joints and fractures can cause an increase in water content, leading to elevated stress levels and a decrease in the strength of soil and rock. As a result, the stability of the soil and rock is reduced [47,48].

3.5. Lithology and Soil

The kind of rock and the extent of chemical and mechanical weathering play a significant role in determining the vulnerability of slopes to landslides [49]. The rock types discovered in Madinah Al Minawarrah are diverse and consist mostly of granites, schists, and gneisses, which are forms of igneous and metamorphic rocks (Figure 5a). This information is based on the field mapping conducted by Johnson and Kattan, 2002. Analyzing the composition and structure of these rocks aids in identifying regions that are susceptible to landslide risks [24]. The existence of granitic rocks enhances the likelihood of landslides. Granitic rocks frequently exhibit extensive fracturing and are susceptible to substantial weathering, resulting in exfoliation and the development of clay particles that diminish the rock's strength. Schists and gneisses exhibit foliation, a property that creates inherent planes of weakness. When foliated planes align parallel to the slope, they function as slip surfaces, greatly diminishing stability, rendering these rocks susceptible to sliding due to gravitational forces, and thus heightening the likelihood of landslides [50]. The rocks along Al Figrah Road exhibit a multitude of joints and foliations, resulting in the formation of planes that are structurally weaker in the rock (Figures 6 and 7). These characteristics typically exhibit a very high propensity for water to seep through, which encourages a more intense process of weathering. As a result, this reduces stability, especially in steep slopes and denudational hills [51].

 doi:10.20944/preprints202410.1125.v1

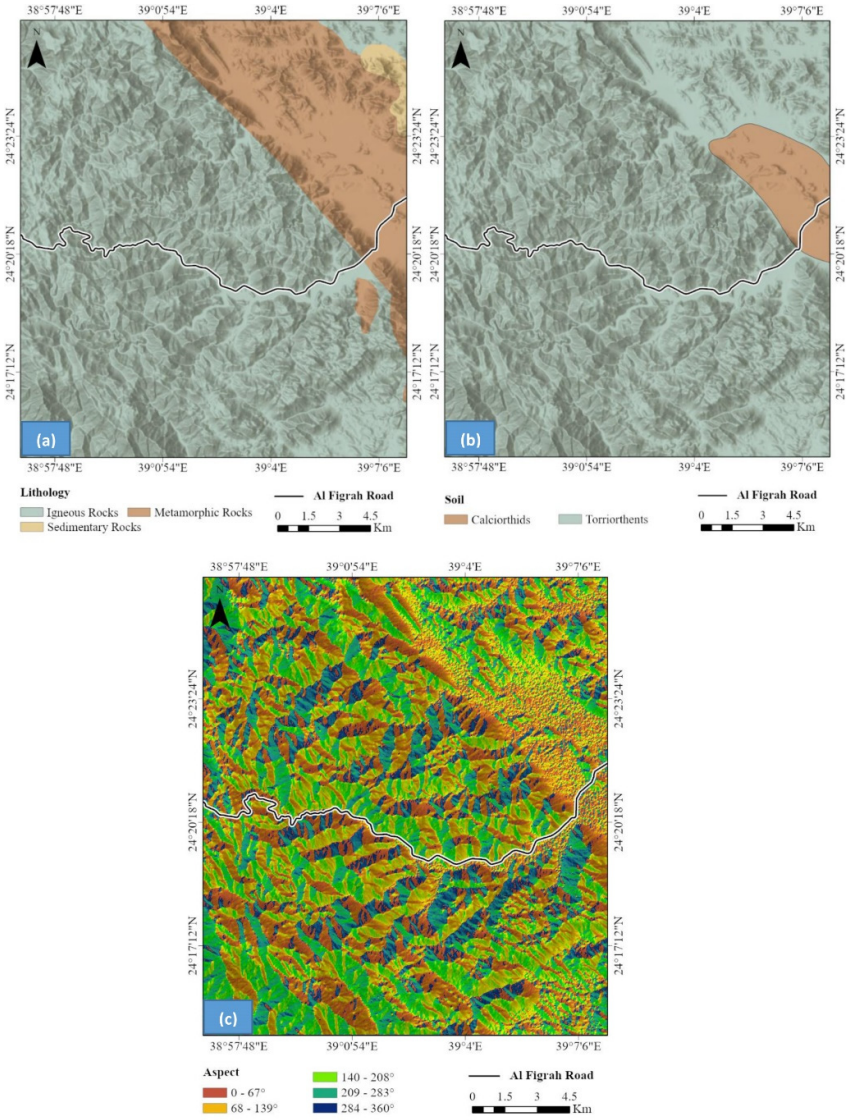

Figure 5. (a) A geological map of the various rock formations presents in the study area. The research region predominantly consists of diorite, granodiorite, granite, and granite gneiss rocks. (b) A map exhibits the arrangement of soil types within the designated area. (c) A map displaying the five distinct directional classes in the designated study area.

 doi:10.20944/preprints202410.1125.v1

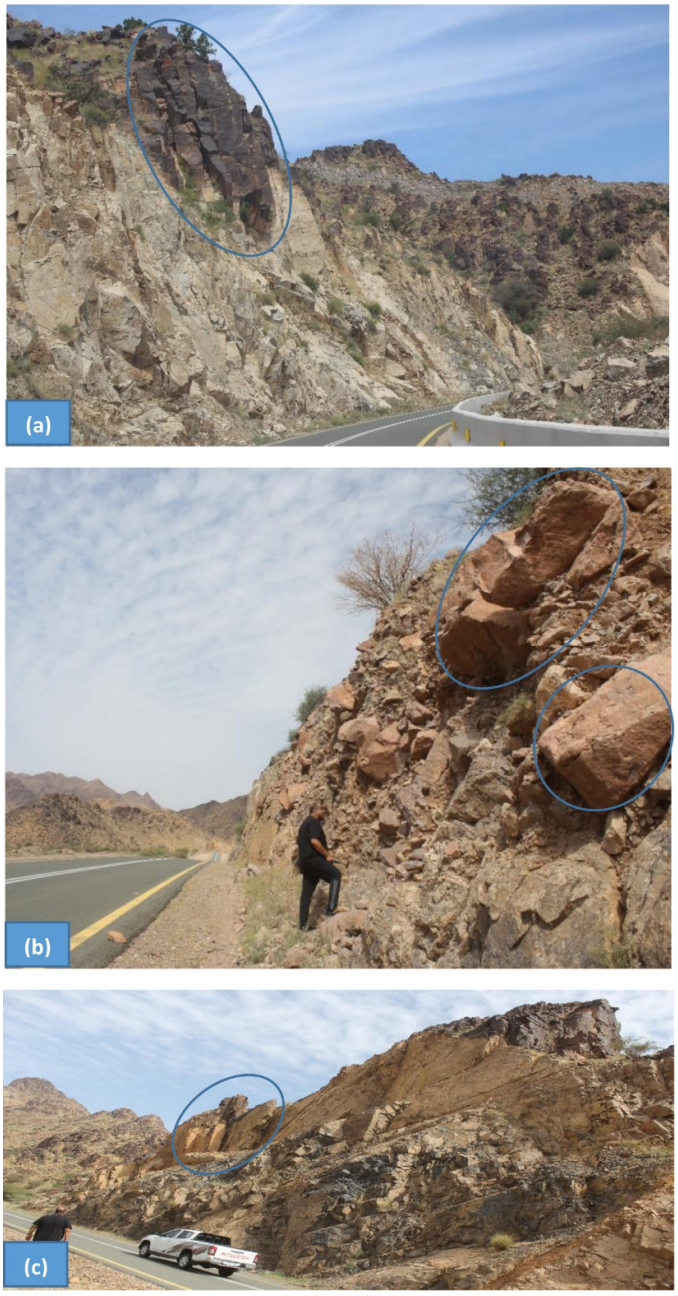

Figure 6. The internal features of rocks and soils that contribute to the occurrence of rock sliding. (a) Rocks that are both jointed and fractured in a hilly environment with steep slopes. (b) Massive granitic slabs sitting on loose rock fragments and earth, poised for sliding. (c) Jointed granitic blocks are prone to sliding when the trigger is present.

 doi:10.20944/preprints202410.1125.v1

Figure 7. The internal structures that are linked to rocks and have a role in causing rock sliding. (a) Fragmented granitic blocks in the process of undergoing exfoliation and sliding. (b) Parallel and perpendicular joints are planes of weakness that can allow water to infiltrate and assist sliding. (c) A fractured granitic block located beside the road.

Soil plays a significant impact in the occurrence of natural disasters, such as floods and landslides [52]. Calciorthids and Torriorthents are the predominant soil types in the research area (Figure 5b). Calciorthids create a layer of soil that contains calcium, which can range in depth and have a texture that is sandy to loamy. This is particularly true in the eastern part of Al Figrah Road. Torriorthents primarily develop on slopes that are undergoing active erosion and in materials that are resistant to weathering. The composition of these soils includes loamy sand, fine sandy loam, sandy loam, loam, or clay loam, as well as their gravelly equivalents [53,54]. The presence of clay in the studied area is a result of the chemical breakdown of granites. This clay content has the potential to create a slip zone, which can lead to slope collapse and landslides, especially in areas with steep terrain [55]. Clayey soil, due to its low permeability and high porosity, has a greater capacity to retain water. This causes a decrease in the soil's shear strength, which ultimately leads to slope failure [56,57].

3.6. Aspect

An aspect map of a research area is crucial for understanding the direction in which the slopes in that region incline. This tool facilitates the identification of areas that are prone to erosion or landslides, particularly in road cuts situated in mountainous topography. Landslide occurrence is

 doi:10.20944/preprints202410.1125.v1

more likely when the structural plane is aligned with the road cuttings [58]. By understanding the dip direction of the slopes, we can improve our capacity to strategically plan activities in the area, ensuring they are carried out safely and efficiently. The aspect data is categorized into five ranges: 0–67° (northeast), 68–139° (northeast–southeast), 140–208° (southeast–southwest), 209–283° (southwest–northwest), and 284–360° (northwest) (Figure 5c).

3.7. Landslide Susceptible Zones and Validation

Field investigations indicated that the predominant threats near Al Figrah Road were rapid downslope landslides that collided with the road. These instances occurred subsequent to severe rainstorms. Intense rainfall on the steep slopes of Al Figrah Mountain can rapidly generate significant surface runoff, which transports loose rocks downhill. In addition, road cuts are a contributing cause to the initiation of landslides. The road works on the slopes of Al Figrah Mountain might lead to substantial disruptions, resulting in instability and the weakening of the slopes. These operations involve the removal of material or the modification of the landscape, which increases the vulnerability of slopes to mass-wasting events like landslides. Furthermore, on-site observations revealed that water flowed across the mountainous terrain after intense precipitation, eventually reaching concentrated drainage zones. Certain locations with high intensity are located on steep slopes and denudational hills in the high-elevation region, namely in the western portion of the research area. In this instance, the geological formations, specifically the igneous and metamorphic joints and foliations, were unstable, resulting in landslides that affected Al Figrah Road.

Table 1 displays the weight percentage for each parameter and the rank of each class, which are various factors that influence the risk of landslide inside the analytic hierarchy process (AHP). The drainage density metric holds the highest weight percentage at 38, indicating that it is the most influential factor in determining the danger of landslide. The slope parameter has a weight % of 32, which is the second highest, while the elevation parameter has a weight percentage of 10, ranking it third. Each of the characteristics—precipitation, lithology, soil, and aspect—has a weight percentage of five, indicating that they have a relatively minor impact on the susceptibility of landslides.

Table 1. The layers utilized in the overlay analysis to identify potential landslide zones and their influences, classes, and scales.

Parameter	Weight (%)	Classes	Rank
Slope (Degree)	32	0–9	1
		10–18	2
		19–26	3
		27–34	4
		35–73	5
Precipitation (mm)	5	45.6–47.3	1
		47.4–48.7	2
		48.8–50	3
		50.1–51.4	4
		51.5–52.9	5
Elevation (m)	10	795–980	1
		981–1153	2
		1154–1335	3
		1336–1524	4
		1525–1866	5
Lithology	5	Igneous Rocks	5
		Metamorphic Rocks	3
		Sedimentary Rocks	1
		Volcanic Rocks	4
Drainage density (km^2)	38	0–0.9	1

 doi:10.20944/preprints202410.1125.v1

		1–1.5	2
		1.6–2.1	3
		2.2–2.8	4
		2.9–4.5	5
Soil	5	Calciorthids	1
		Torriorthents	2
Aspect	5	0–67° (NE)	1
		68–139° (NE–SE)	2
		140–208° (SE–SW)	3
		209–283° (SW–NW)	4
		284–360° (NW)	5

Figure 8 illustrates the results of the AHP study, indicating the locations with different degrees of landslide risk. It is worth mentioning that the previous landslides were mainly concentrated in the high-elevation area. The low-risk zones are denoted by the color green, including a total area of 93,552,333 m^2. The locations with a moderate level of danger are designated by the color yellow and have a total area of 271,180,722 m^2. The areas with a high level of risk are shown in the color red, and they encompass a total area of 33,053,839 m^2.

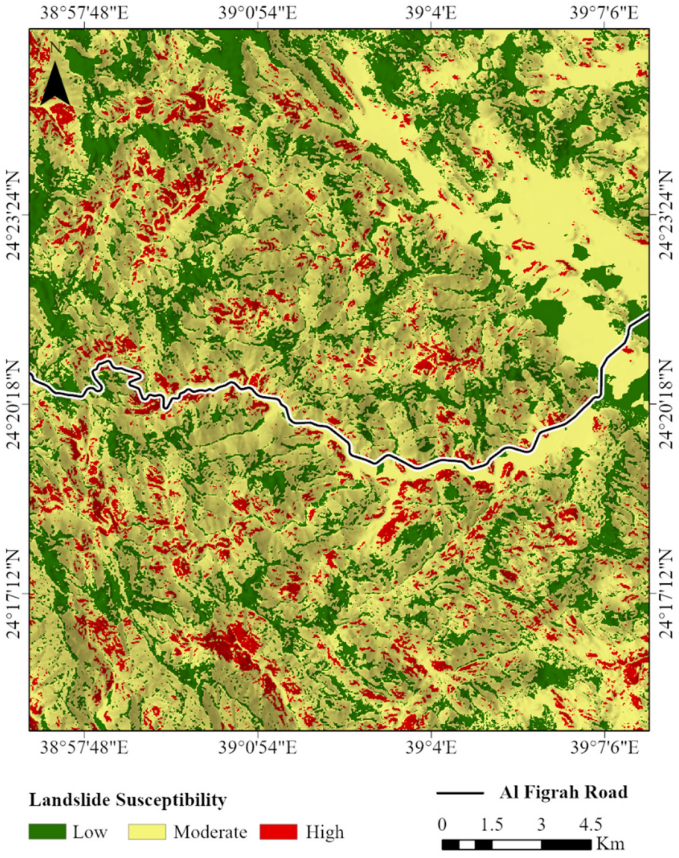

Figure 8. Map displaying the potential landslide zones in the Al Figrah Road area.

Excavating slopes for road construction and expansion is a frequent practice in hilly areas, and it has a notable influence on the stability of the slopes [59,60]. The current work employs remote sensing data and leverages AHP analysis technologies in the GIS environment to detect past landslide occurrences and forecast likely future landslide locations. During the field trip, a total of 10 landslide

 doi:10.20944/preprints202410.1125.v1

spots were identified and utilized to verify the risk zones generated for the current study (Figure 7). This preventive measure is crucial for eliminating any erroneous results. All ten landslides occurred in the high-risk areas, confirming the findings of the AHP research. Regarding Al Figrah Road, out of the overall 26.2 kilometer route, 7.5 km is classified as low risk, 12.6 km as moderate risk, and 6.1 km as high danger.

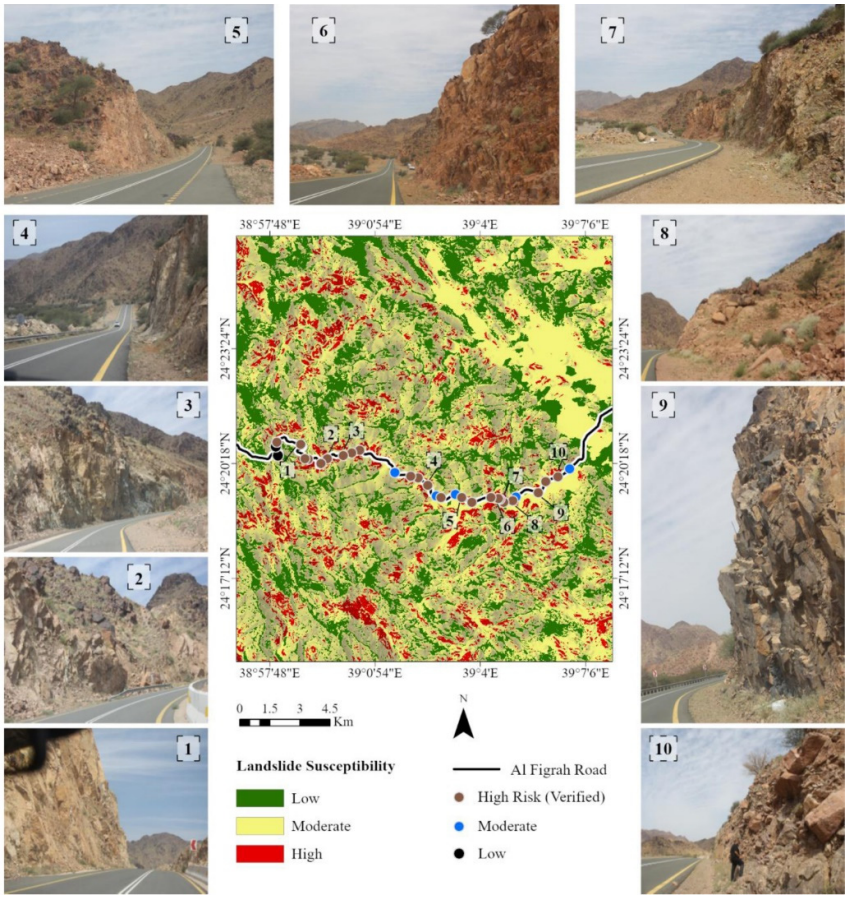

Figure 7. Potential landslide zones resulting from analytic hierarchy process (AHP) and the 10 observed landslides from the field trip to Al Figrah Mountain. The figure demonstrates the validity of the proposed AHP method for assessing landslide hazards in the study area.

5. Conclusions

The current study utilized GIS-based analytic hierarchy process (AHP) and remote sensing data to create a landslide susceptibility map for the Al Figrah Mountain region in western Saudi Arabia. The study employed multiple characteristics, including drainage density, elevation, slope, precipitation, lithology, soil, and aspect, to delineate the landslide zones in the region. The assessment revealed that the low-risk areas encompass 23.52% of the research area, while moderate-risk areas account for 68.17%, and high-risk areas make up 8.31%. The excursion to Al Figrah Road revealed the presence of 10 past occurrences of landslides in regions distinguished by abundant water drainage and a steep incline. The Al Figrah Road can be divided into three categories based on risk levels: 28.63% is classified as low risk, 48.09% as moderate risk, and 23.28% as high danger. This work establishes a fundamental starting point for future investigations on landslides and risk assessment in Saudi Arabia and other comparable regions. Additional investigation is required to comprehend the potential impact of climate change on landslides in the mountainous regions of Saudi Arabia.

Author Contributions: Conceptualization, T.A. and A.S.E.-S.; methodology, T.A. and A.S.E.-S.; software, T.A. and A.S.E.-S.; writing—original draft preparation, T.A. and A.S.E.-S.; writing—review and editing, T.A. and A.S.E.-S. All authors have read and agreed to the published version of the manuscript.

Funding: Researchers' supporting project number (RSPD2023R791), King Saud University, Riyadh, Saudi Arabia.

Institutional Review Board Statement:

Informed Consent Statement:

Data Availability Statement: All data generated or analyzed during this study are included in the published article.

Acknowledgments: The authors extend their appreciation to Researchers Supporting Project number (RSPD2023R791), King Saud University, Riyadh, Saudi Arabia. Moreover, the authors thank the anonymous reviewers for their valuable suggestions and constructive comments.

Conflicts of Interest: The authors declare no conflicts of interest.

References

1. Luo, H.Y.; Zhang, L.M.; Zhang, L.L.; He, J.; Yin, K.S. Vulnerability of buildings to landslides: The state of the art and future needs. *Earth-Sci. Rev.* **2023**, *238*, 104329.
2. Reichenbach, P.; Rossi, M.; Malamud, B.D.; Mihir, M.; Guzzetti, F. A review of statistically-based landslide susceptibility models. *Earth-Sci. Rev.* **2018**, *180*, 60–911.
3. Lacroix, P.; Handwerger, A.L.; Bièvre, G. Life and death of slow-moving landslides. *Nat. Rev. Earth Environ.* **2020**, *1*, 404–419.
4. Alharbi, T.; Sultan, M.; Sefry, S.; ElKadiri, R.; Ahmed, M.; Chase, R An assessment of landslide susceptibility in the Faifa area, Saudi Arabia, using remote sensing and GIS techniques. *Nat. Hazards Earth Syst. Sci.* **2014**, *14*, 1553–1564.
5. Zhou, W.; Qiu, H.; Wang, L.; Pei, Y.; Tang, B.; Ma, S.; Yang, D.; Cao, M. Combining rainfall-induced shallow landslides and subsequent debris flows for hazard chain prediction. CATENA 2022, 213, 106199.
6. Qiu, H.; Zhu, Y.; Zhou, W.; Sun, H.; He, J.; Liu, Z. Influence of DEM resolution on landslide simulation performance based on the SCOOPS3D model. Geomatics, Natural Hazards and Risk 2022, 13, 1663–1681.
7. Casagli, N.; Intrieri, E.; Tofani, V.; Gigli, G.; Raspini, F. Landslide detection, monitoring and prediction with remote-sensing techniques. Nat. Rev. Earth Environ. 2023, 4, 51–64.
8. Chauhan, S., Sharma, M., Arora, M.K., 2010. Landslide susceptibility zonation of the Chamoli region, Garhwal Himalayas, using logistic regression model. Landslides 7(4), 411–423. https://doi.org/10.1007/s10346-010-0202-3.
9. Jim'enez-Per´alvarez, J.D., Irigaray, C., El Hamdouni, R., Chac´on, J., 2009. Building models for automatic landslide-susceptibility analysis, mapping and validation in ArcGIS. Nat. Hazards 50 (3), 571–590. https://doi.org/10.1007/s11069-008-9305- 8.
10. Meten, M., PrakashBhandary, N., Yatabe, R., 2015. Effect of landslide factor combinations on the prediction accuracy of landslide susceptibility maps in the Blue Nile Gorge of Central Ethiopia. Geoenviron. Disasters 2 (1). https://doi.org/ 10.1186/s40677-015-0016-7.
11. Singh, S., Dhote, P.R., Thakur, P.K., Chouksey, A., Aggarwal, S.P., 2021. Identification of flash-floods-prone river reaches in Beas river basin using GIS-based multi-criteria technique: validation using field and satellite observations. Nat. Hazards 105 (3), 2431–2453. https://doi.org/10.1007/s11069-020-04406-w.
12. Park, S., Choi, C., Kim, B., Kim, J., 2013. Landslide susceptibility mapping using frequency ratio, analytic hierarchy process, logistic regression, and artificial neural network methods at the Inje area, Korea. Environ. Earth Sci. 68 (5), 1443–1464.
13. Yalcin, A., Reis, S., Aydinoglu, A., Yomralioglu, T., 2011b. A GIS-based comparative study of frequency ratio, analytical hierarchy process, bivariate statistics and logistics regression methods for landslide susceptibility mapping in Trabzon, NE Turkey. Catena 85 (3), 274–287. https://doi.org/10.1016/j.catena.2011.01.014.
14. Guzzetti, F., Carrara, A., Cardinali, M. & Reichenbach, P. 1999. Landslide hazard evaluation: A review of current techniques and their application in a multi-scale study, Central Italy. Geomorphology 31, 181–216.
15. Peng, J. et al., 2019. Distribution and genetic types of loess landslides in China. J. Asian Earth Sci. 170, 329–350. https:// doi. org/ 10. 1016/j.jseaes. 2018. 11. 015.
16. Liu, X., Shao, S., Shao, S., 2024. Landslide susceptibility zonation using the analytical hierarchy process (AHP) in the Great Xi'an Region, China. Scientific Reports, 14, 2941. https://doi.org/10.1038/s41598-024-53630-y

17. Xiong, T., Indrawan, G.B., Putra, D.P., 2017. Landslide Susceptibility Mapping Using Analytical Hierarchy Process, Statistical Index, Index of Enthropy, and Logistic Regression Approaches in the Tinalah Watershed, Yogyakarta. Journal of Applied Geology, 2(1), 66–82 DOI: http://dx.doi.org/10.22146/jag.30
18. Shu, H. et al., 2021. Integrating landslide typology with weighted frequency ratio model for landslide susceptibility mapping: A case study from Lanzhou city of northwestern China. Remote Sens. 13, 3623.
19. Zhou, J.; Tan, S.; Li, J.; Xu, J.; Wang, C.; Ye, H. Landslide Susceptibility Assessment Using the Analytic Hierarchy Process (AHP): A Case Study of a Construction Site for Photovoltaic Power Generation in Yunxian County, Southwest China. Sustainability 2023, 15, 5281. https://doi.org/10.3390/su15065281
20. Haque, U., Da Silva, P. F., Devoli, G., Pilz, J., Zhao, B., Khaloua, A., ... & Glass, G. E. (2019). The human cost of global warming: Deadly landslides and their triggers (1995–2014). Science of the Total Environment, 682, 673-684.
21. Dikshit, A., Sarkar, R., Pradhan, B., Segoni, S., & Alamri, A. M. (2020). Rainfall induced landslide studies in Indian Himalayan region: a critical review. Applied Sciences, 10(7), 2466.
22. Youssef, A. M. (2013). Landslide susceptibility mapping using GIS and remote sensing techniques in the Abha area, Asir region, Saudi Arabia. Arabian Journal of Geosciences, 6(8), 2949–2961. https://doi.org/10.1007/s12517-012-0574-7
23. Youssef, A. M., Al-Kathery, M., & Pradhan, B. (2015). Landslide susceptibility mapping at Al-Hasher area, Jizan (Saudi Arabia) using GIS-based frequency ratio and index of entropy models. Geosciences Journal, 19, 113-134.
24. Alharbi, T.; El-Sorogy, A.S. Landslide Prediction in Mountainous Terrain Using Remote Sensing and GIS: A Case Study of Al-Hada Road, Makkah Province, Saudi Arabia. Water **2023**, 15, 3771. https://doi.org/10.3390/w15213771
25. Youssef, A.M.; Mahdi, A.M.; Al-Katheri, M.M.; Pouyan, S.; Pourghasemi, H.R. Multi-hazards (landslides, floods, and gully erosion) modeling and mapping using machine learning algorithms. J. Afr. Earth Sci. 2023, 197, 104788.
26. Sadagah, B. A vigorous debris-flow incident at Al-Hada descent and remedial measures. In *Landslide Science for a Safer Geoenvironment*; Sassa, K., Canuti, P., Yin, Y., Eds.; Springer: Berlin/Heidelberg, Germany, 2014; pp. 715–718.
27. Stüwe, K.; Robl, J.; Turab, S.A.; Sternai, P.; Stuart, F.M. Feedbacks between sea-floor spreading, trade winds and precipitation in the Southern Red Sea. Nat. Commun. 2022, 13, 5405.
28. Almazroui, M.; Islam, M.N.; Alkhalaf, A.K.; Saeed, F. Spatiotemporal analysis of the annual rainfall in the Kingdom of Saudi Arabia. Theor. Appl. Climatol. 2021, 144, 1039–1054.
29. Ma, S.; Qiu, H.; Zhu, Y.; Yang, D.; Tang, B.; Wang, D.; Wang, L.; Cao, M. Topographic changes, surface deformation and movement process before, during and after a rotational landslide. Remote Sens. 2023, 15, 662.
30. Hürlimann, M.; Coviello, V.; Bel, C.; Guo, X.; Berti, M.; Graf, C.; Hübl, J.; Miyata, S.; Smith, J.B.; Yin, H.Y. Debris-flow monitoring and warning: Review and examples. Earth-Sci. Rev. 2019, 199, 102981.
31. Amin, A. A., & Mesaed, A. A. The Role of the Geologic and the Geomorphologic Factors in the Formation of Some Geotourism Sites of Saudi Arabia. In Geotourism in the Middle East, 2023, (pp. 193-234). Cham: Springer International Publishing.
32. Climate-Data.org. Medina climate: Average Temperature, weather by month, Medina weather averages—Climate-Data.org. Available online: https://en.climate-data.org/asia/saudi-arabia/al-madinah-region/medina-3534/ (accessed on 17 June 2024).
33. Aldrees, A. Climatic impact on Rainfall Analysis in Al-Madinah Munawwara Region. In IOP Conference Series: Earth and Environmental Science (Vol. 1026, No. 1, p. 012032). IOP Publishing. 2022.
34. Zhang, Q.; Ye, S.; Yan, F.; Ren, B. Application of RS & GIS in Regional Landslides Susceptibility Mapping and Spatiotemporal Characteristics Analysis. IOP Conf. Ser. Earth Environ. Sci. 2020, 428, 012093.
35. Tavana, M., Soltanifar, M., & Santos-Arteaga, F. J. Analytical hierarchy process: revolution and evolution. Annals of operations research, 326(2), 879-907. 2023
36. Yousefi, H., Moradi, S., Zahedi, R., & Ranjbar, Z. Developed analytic hierarchy process and multi criteria decision support system for wind farm site selection using GIS: A regional-scale application with environmental responsibility. Energy Conversion and Management: X, 22, 100594. 2024
37. Alharbi, T., A Weighted Overlay Analysis for Assessing Urban Flood Risks in Arid Lands: A Case Study of Riyadh, Saudi Arabia. Water, 16(3), 397, 2024.
38. Alharbi, T. Mapping of groundwater, flood, and drought potential zones in neom, Saudi Arabia, using GIS and remote sensing techniques. *Water* **2023**, *15*, 966.
39. Lin, P.; Pan, M.; Wood, E.F.; Yamazaki, D.; Allen, G.H. A new vector-based global river network dataset accounting for variable drainage density. Sci. Data 2021, 8, 28. https://doi.org/10.1038/s41597-021-00819-9.
40. Yang, S.-Y.; Chang, C.-H.; Hsu, C.-T.; Wu, S.-J. Variation of uncertainty of drainage density in flood hazard mapping assessment with coupled 1D–2D hydrodynamics model. Nat. Hazards 2022, 111, 2297–2315. https://doi.org/10.1007/s11069-021-05138-1.

41. Liu, C.; Wang, J.; Li, Z. A new method for estimating the potential energy of debris flows based on a two-phase flow model. Landslides 2019, 16, 1–14. https://doi.org/10.1007/s10346-018-1075-0.
42. Hengl, T.; Reuter, H.I. (Eds.). Geomorphometry: Concepts, Software, Applications; Elsevier: Amsterdam, The Netherlands, 2009; Chapter 2: Digital elevation model terminology.
43. Zhou, Q.; Liu, X. Analysis of errors of derived slope and aspect related to DEM data properties. *Comput. Geosci.* **2004**, *30*, 369-378. https://doi.org/10.1016/j.cageo.2003.11.016.
44. Gabet, E.J.; Mudd, S.M. Bedrock erosion by root fracture and tree throw: A coupled biogeomorphic model to explore the humped soil production function and the persistence of hillslope soils. *J. Geophys. Res. Earth Surf.* **2010**, *115*. https://doi.org/10.1029/2009JF001526.
45. Larsen, I.J.; Montgomery, D.R. Landslide erosion coupled to tectonics and river incision. *Nat. Geosci.* **2012**, *5*, 468–473. https://doi.org/10.1038/ngeo1479.
46. Panchal, S.; Shrivastava, A.K. Landslide hazard assessment using analytic hierarchy process (AHP): A case study of National Highway 5 in India. Ain Shams Eng. J. 2022, 13, 101626.
47. Yalcin, A. The effects of clay on landslides: A case study. Appl. Clay Sci. 2007, 38, 77–85.
48. Temme, A.J.A.M. Relations between soil development and landslides. In Hydrogeology, Chemical Weathering, and Soil Formation; Hunt, A., Egli, M., Faybishenko, B., Eds.; American Geophysical Union: Washington, DC, USA, 2021.
49. Xiong, H., Ma, C., Li, M., Tan, J. & Wang, Y., 2023. Landslide susceptibility prediction considering land use change and human activity: A case study under rapid urban expansion and afforestation in China. Sci. Total Environ. 866, 161430.
50. Stern, R.J., & Johnson, P.R. (2010). Continental Lithosphere of the Arabian Plate: A Geologic, Petrologic, and Geophysical Synthesis. Earth-Science Reviews, 101(1-2), 29-67.
51. Twiss, R.J., & Moores, E.M. (2007). Structural Geology. W.H. Freeman and Company.
52. Borrelli, P.; Robinson, D.A.; Panagos, P.; Lugato, E.; Yang, J.E.; Alewell, C.; Wuepper, D.; Montanarella, L.; Ballabio, C. Land use and climate change impacts on global soil erosion by water (2015–2070). *Proc. Natl. Acad. Sci. USA* **2020**, *117*, 21994–22001. https://doi.org/10.1073/pnas.2001403117.
53. Ministry of Agriculture and Water (MAW). General soil map of the Kingdom of Saudi Arabia. Ministry of Agriculture and Water, Land Management Department, 1985.
54. Sheta, A.S. Soil quality: Standards of soil quality under the conditions of Saudi Arabia, 7th ed.; Saudi Society for Agricultural Sciences, King Saud University: Riyadh, Saudi Arabia, 2004. (In Arabic)
55. Sur, U.; Singh, P.; Meena, S.R. Landslide susceptibility assessment in a lesser Himalayan Road corridor (India) applying fuzzy AHP technique and earth-observation data. Geomat. Nat. Hazards Risk 2020, 11, 2176–2209.
56. Chawla, A.; Chawla, S.; Pasupuleti, S.; Rao, A.C.S.; Sarkar, K.; Dwivedi, R. Landslide susceptibility mapping in Darjeeling Himalayas, India. Adv. Civ. Eng. 2018, 2018, 6416492.
57. Thomas, A.V.; Saha, S.; Danumah, J.H.; Raveendran, S.; Prasad, M.K.; Ajin, R.S.; Kuriakose, S.L. Landslide susceptibility zonation of Idukki district using GIS in the aftermath of 2018 Kerala floods and landslides: A comparison of AHP and frequency ratio methods. J. Geovis. Spat. Anal. 2021, 5, 21.
58. Saravanan, S.; Thirumalaivasan, D. Assessment of Morphometric Parameters as the Basis for Hydrological Analysis of a River Basin Using GIS and Remote Sensing Techniques. ISPRS Int. J. Geo-Inf. 2020, 11, 459. https://doi.org/10.3390/ijgi11090459.
59. Sharma, S.; Mahajan, A.K. Comparative evaluation of GIS-based landslide susceptibility mapping using statistical and heuristic approach for Dharamshala region of Kangra Valley, India. Geoenviron. Disasters 2018, 5, 4.
60. Singh, K.; Sharma, A. Road cut slope stability analysis at Kotropi landslide zone along NH-154 in Himachal Pradesh, India. J. Geol. Soc. India 2022, 98, 379–386.